Organometallics **2003,** *22,* 5047−5053 5047

Electronic Control of the Asymmetry in Heteroatom Monosubstituted Olefin Bonding to the Cyclopentadienyl Iron(II) Dicarbonyl Cation. A Hammett Correlation Study

Stephen A. Matchett,* Brenda R. Schmiege-Boyle,‡ John Cooper,‡
David Fratterelli,‡ Kirk Olson,‡ Justin Roberts,‡ James Thommen,‡
Dean Tigelaar,‡ and Frederique Winkler‡

Department of Chemistry, Grand Valley State University, Allendale, Michigan 49401

Received July 28, 2003

Nucleophilic substitution of $CpFe(CO)_2(\eta^2\text{-}H_2CC(H)OEt)^+PF_6^-$ with para-substituted anilines was used to prepare a series (**4**−**10**) of η^2-vinyl aniline Fp^+ complexes of the general formula $CpFe(CO)_2[\eta^2\text{-}CH_2C(H)NH(p\text{-}C_6H_4X)]^+PF_6^-$, where X = OMe (**4**), Me (**5**), H, (**6**), Br (**7**), COMe (**8**), CN (**9**), and NO_2 (**10**). Correlation of the Hammett σ para parameters with the ^{13}C NMR shifts of the metal-coordinated vinyl carbons demonstrated the ability to control the position of the Fp^+ moiety along the olefin face. As the electron-donating character of the para substituent was increased, the Fp^+ moiety was displaced away from the nitrogen-bearing carbon, increasing the asymmetry of the metal−olefin bonding. These conclusions were further supported by determining the X-ray crystal structure of the *p*-Me (**5**) and the *p*-acetyl (**8**) derivatives.

Introduction

Interest in the nature of metal−olefin bonding and its effect on olefin reactivity finds relevance in organotransition metal mediated organic synthesis as well as polymer synthesis.[1] The Chatt−Dewar−Duncanson model[2] describes the metal−olefin bond as a combination of σ donation from the olefin to the metal and a π back-bond from the metal into the π^* orbital on the olefin. Metal−olefin complexes range in structure from purely symmetric to highly distorted structures that demonstrate significant reduction in the carbon−carbon bond order.

In cases where the metal acts predominately as a σ acid, conventional olefin chemistry can be reversed, activating the olefin to nucleophilic attack.[3] In the early 1980s, calculations on a series of metal ethylene complexes by Hoffmann and Eisenstein[4] sought to explain the source of this activation. They concluded that a distortion of the symmetric structure wherein the metal fragment slides along the face of the olefin to favor one side (hereafter referred to as the α carbon) results in a stabilization and localization of a carbon-centered LUMO on the opposite (β) carbon. This displacement of the metal makes this developing LUMO available for overlap with an incoming nucleophile. They quantified the extent of the displacement in their calculations by the parameter Δ, defined as the horizontal displacement of the metal away from the center of the olefin face.

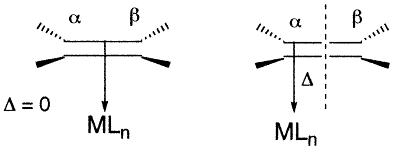

They concluded that as Δ approached a distance reflecting a loss of the η^2 olefin structure in favor of an η^1 σ interaction of the metal and the α carbon (0.69 Å), the olefin became activated to nucleophilic attack at the β carbon.

Displacement of the metal along the olefin face can also occur in the ground state structure as a result of the olefin substituents. Rosenblum and co-workers[5] reported a series of iron olefin complexes that explored the structural consequences of heteroatom substitution on the coordinated olefin. Comparison of the structures of **1** ($[(\eta^5\text{-}C_5H_5)Fe(CO)_2(\eta^2\text{-}C_2H_4)]^+PF_6^-$), **2** ($[(\eta^5\text{-}C_5H_5)Fe(CO)_2(\eta^2\text{-}CH_2CHOCH_3)]^+PF_6^-$), and **3** ($[(\eta^5\text{-}C_5H_5)Fe(CO)_2$-

---

* To whom correspondence should be addressed. E-mail: matchets@gvsu.edu.

‡ Contributed as undergraduate researchers at Grand Valley State University.

[1] Numerous references can be traced through the following texts. (a) Collman, J. P.; Hegedus, L. S.; Norton, J. R.; Finke, R. G. *Principles and Applications of Organotransition Metal Chemistry*; Univerity Science Books: Mill Valley, CA, 1987; Chapters 11, 17, 19, 20. (b) Hegedus, L. S. *Transition Metals in the Synthesis of Complex Organic Molecules*; University Science Books, Mill Valley, CA, 1994; Chapters 7 and 9.

[2] Dewar, M. J. S. *Bull. Soc. Chim. Fr.* **1951**, *18*, C71−C79; *Annu. Rep. Prog. Chem.* **1951**, *48*, 112−135. Chatt, J.; Duncanson, L. A. *J. Chem. Soc.* **1953**, 2239−2947.

[3] Examples are numerous, including: (a) Green, M. L. H.; Naagy, P. L. I. *J. Organomet. Chem.* **1963**, *1*, 58. And specific to Fp$^+$olefin complexes: (b) Chang, T. C. T.; Rosenblum, M. *Isr. J. Chem.* **1984**, *24*, 99. (c) Lennon, P.; Madhavarao, M.; Rosan, A.; Rosenblum, M. *J. Organomet. Chem.* **1976**, *108*, 93. (d) Marsi, M.; Rosenblum, M. *J. Am. Chem. Soc.* **1984**, *106*, 7264. (e) Chang, T. C. T.; Rosenblum, M.; Samuels, S. B. *J. Am. Chem. Soc.* **1980**, *102*, 5931.

[4] (a) Eisenstein, O.; Hoffmann, R. *J. Am. Chem. Soc.* **1980**, *102*, 6148. (b) Eisenstein, O.; Hoffmann, R. *J. Am. Chem. Soc.* **1981**, *103*, 4308.

[5] Chang, T. C. T.; Foxman, B. M.; Rosenblum, M.; Stockman, C. *J. Am. Chem. Soc.* **1981**, *103*, 7361.

10.1021/om0305566 CCC: $25.00

(η^2-CH_2CHNMe_2)]$^+PF_6^-$) revealed an increasing ground state displacement of the iron toward the α carbon across the series.

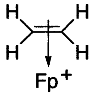

1

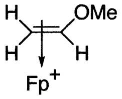

2

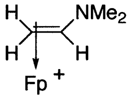

3

Where Fp$^+$ = $CpFe(CO)_2^+$

Rosenblum proposed[5] that donation from the heteroatom lone pair could be stabilizing the β carbon LUMO predicted by Hoffmann and Eisenstein,[4] yielding the displacements seen in their series.[6] It was reasoned that the greater displacement seen in **3** was due to better overlap between the lone pair on nitrogen (vs oxygen) with the potential LUMO on the β carbon. As such, the electronic structure of these complexes can be thought of as points along a continuum between the following two resonance structures (I and II) where X is a heteroatom.

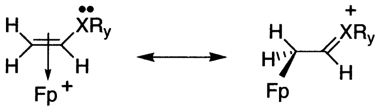

I **II**

The position along the continuum should therefore be a function of the energy match between the heteroatom lone pair and the developing β carbon-centered LUMO.

The presence of a heteroatom lone pair is not enough to ensure a displacement of the metal along the olefin face. If the metal fragment acts as a good π base, these distortions of the metal–olefin bonding are reduced or not observed. For example, neither the η^2-vinyl ether[7] or the η^2-2,5-dimethyl pyrrole complex[8] of $Os(NH_3)_5^{+2}$ shows any significant distortion from symmetrical olefin binding.[9]

The chemical consequences of this displacement are manifest in the relative reactivity of the complexed olefin to nucleophilic attack. Rosenblum suggested that some stabilization of the LUMO by the heteroatom lone pair greatly increases the rate of nucleophilic attack (**2** was reported[5] to be 530 times more reactive than **1** to the same nucleophile). If this stabilization becomes too great (i.e., the displacement of the Fe is too large), the reactivity toward nucleophiles passes through a maximum and then greatly decreases (**3** was virtually unreactive[5]). This suggested to us that one could control the relative energy of the heteroatom lone pair through appropriate substitution and hence tune the chemistry of the olefin.

Herein, we report the synthesis and characterization of a series of seven complexes, analogous to **3**, in which the NMe_2 group is replaced by various para-substituted anilines. The X-ray crystal structure of two of these complexes is reported to place these compounds in the context of the known complexes **1**–**3**. Finally, a correlation between Hammett σ_{para} parameters and the ^{13}C NMR shifts of the carbons of the complexed olefin is established. This correlation experimentally supports the proposed influence of the heteroatom lone pair on metal–olefin bonding. Thus, the position along the continuum between resonance structures I and II can be tuned by the functionality of the para substituent, allowing for systematic control over the metal olefin structure and potentially over its chemistry.

Results and Discussion

Using the known susceptibility of cyclopentadienyl iron dicarbonyl (hereafter referred to as Fp) vinyl ether complexes to nucleophilic substitution,[10] we prepared a series of para-substitued aniline analogues of compound **3** according to the reaction shown (where X was OMe, Me, Br, H, COMe, CN, and NO_2). Each derivative forms readily in CH_2Cl_2 solution by treatment of the ethyl vinyl ether compound [$CpFe(CO)_2(CH_2CHOEt)^+$-PF_6^-][11] with a slight molar excess of the para-substituted aniline as the nucleophile. The products are orange to orange-brown solids that precipitate from solution as the reaction proceeds. Reaction time varies with the nucleophilicity of the aniline derivative, but even reactions involving the para nitro derivative are essentially complete within 3–4 h at room temperature.

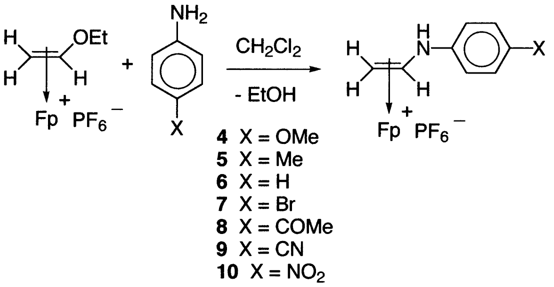

Crystallographic Data on 5 and 8. A single-crystal X-ray diffraction structure was obtained for both complex **5** and complex **8**. Crystals of both complexes (dark red triclinic crystals of **5** and orange-red orthorhombic crystals of **8**) were grown from CH_2Cl_2 solutions layered with diethyl ether. The molecular structures of **5** and **8** are shown in Figures 1 and 2, respectively. Table 1 compares selected bond lengths in these complexes with their analogues in **2** and **3**. The solution of the structure of **5** gave two molecules in the asymmetric unit. These structures differ in some regions of the molecule due to hydrogen bonding and crystal-packing forces in the solid state.[12] Bond lengths for each unique structure are given

---

(6) Participation of the heteroatom lone pair has also been invoked to explain the distortion in the metal–olefin bonding seen in a Pt vinyl alcohol complex. Cotton, F. A.; Francis, J. N.; Frenz, B. A.; Tsutsui, M. *J. Am. Chem. Soc.* **1973**, *95*, 2483.

(7) Chen, H.; Harman, W. D. *J. Am. Chem. Soc.* **1996**, *118*, 5672. Although parts of the X-ray crystal structure were reported to be badly disordered, the geometry around the metal–olefin bonding was clearly resolved.

(8) Myers, W. H.; Sabat, M.; Harman, W. D. *J. Am. Chem. Soc.* **1991**, *113*, 6682.

(9) This is reflected in a reversal in the chemistry with these Os complexes activating the olefin to electrophilic, not nucleophilic attack. See ref 7.

(10) (a) Rosenblum, M. *Acc. Chem. Res.* **1974**, *7*, 122. (b) Chang, T. C. T.; Rosenblum, M.; Samuels, S. B. *J. Am. Chem. Soc.* **1980**, *102*, 5931. (c) Marsi, M.; Rosenblum, M. *J. Am. Chem. Soc.* **1984**, *106*, 7266. (d) Rosenblum, M.; Bucheister, A.; Chang, T. C. T.; Cohen, M.; Marsi, M.; Samuels, S. B.: Scheck, D.; Sofen, N.; Watkins, J. C. *Pure Appl. Chem.* **1984**, *56*, 129, and references therein.

(11) Cutler, A.; Raghu, S.; Rosenblum, M. *J. Organomet. Chem.* **1974**, *77*, 381.

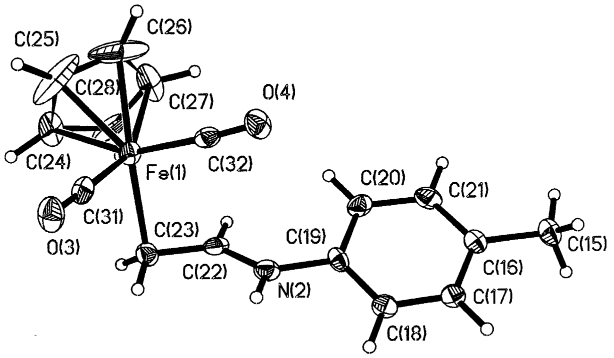

Figure 1. ORTEP drawing showing the molecular structure of **5.** The thermal ellipsoids were set at the 30% probability level. For clarity, only one (**5a**) of the two molecules in the asymmetric unit is shown. ORTEP drawings and full data sets for both molecules are available as Supporting Information. The PF_6^- counterion was removed for further clarity. Selected bond lengths and angles are given in Tables 1 and 2.

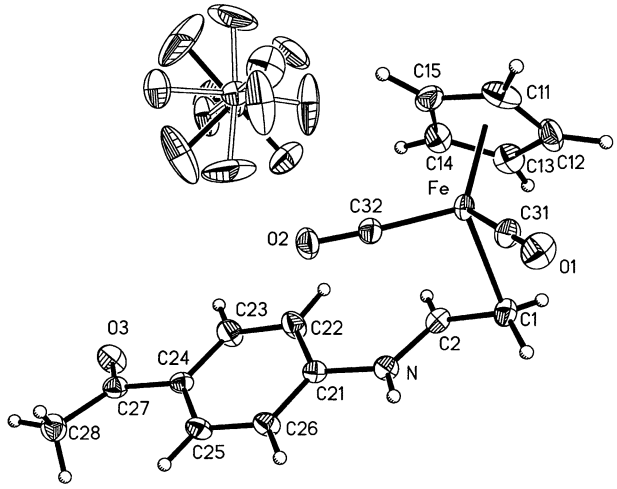

Figure 2. ORTEP drawing showing the molecular structure of **8**. The thermal ellipsoids were set at the 30% probability level. Selected bond lengths and angles are given in Tables 1 and 2.

Table 1. Comparison of Selected Bond Lengths (Å) Relevant to the Displacement of Iron along the Olefin Face in Complexes 2, 3, 5, and 8

	2	**3**	**5a**	5**b**	**8**
$C_\alpha-C_\beta$ olefin bond	1.42(2)	1.408(8)	1.394(6) av = 1.400(7)	1.405(7)	1.385(4)
$Fe-C_\alpha$	2.09(2)	2.121(5)	2.126(5) av = 2.123(5)	2.121(5)	2.164(4)
$Fe-C_\beta$	2.32(2)	2.819(5)	2.582 av = 2.624	2.667	2.518(3)
δ value $[(Fe-C_\beta)-(FeC_\alpha)]$	0.23[a]	0.70	0.456 av = 0.501	0.546	0.354
heteroatom$-C_\beta$	1.34(2)	1.295(7)	1.327(6) av = 1.322(6)	1.317 (6)	1.335(4)
N$-$ring C	NA	NA	1.418(6) av = 1.420(6)	1.422 (6)	1.412(3)

in Table 1, along with their average, which may be more representative of the solution phase structure. Table 2 provides a similar analysis of selected bond angles again with the multiple entries for **5**.

Table 2. Comparison of Selected Bond Angles[a] in Complexes 5 and 8

	5a	**5b**	**8**
$Fe-C_\alpha-C_\beta$	92.0(3)° av = 94.1(3)°	96.1(3)°	87.3(2)°
$C_\beta-N-C_{ring}$	128.5(5)° av = 127.9(5)°	127.3 (5)°	127.2(2)°
dihedral angle between imine and plane of the aniline ring: $C_\beta-N-C-C$	−165.9° av = −163.1°	−160.2°	−178.3°
dihedral angle between olefin and aniline: $C_\alpha-C_\beta-N-C_{ring}$	−170.5° av = −173.0°	−175.5°	170.1°

[a] The dihedral angles were determined by importing the pdb files for each structure into MacSpartan Plus (v 1.04) molecular modeling software and measuring in the molecule editor.

Structures of **5** and **8** provide a direct illustration of the influence of the para substituent on the displacement of the iron along the olefin face. To provide a basis of comparison, we use the Rosenblum δ parameter[5] listed in Table 1, which is equal to the $Fe-C_\beta$ distance minus the $Fe-C_\alpha$ distance. The δ parameter is used in place of the Hoffmann Δ because the former is more easily determined directly from the X-ray crystal structure data. The value of δ equals zero for a symmetric olefin and gets larger as the iron atom is displaced toward the α carbon. Comparing δ values for **2** and **3**, the extent of this displacement is more pronounced for the amine-substituted olefin, in keeping with the proposed[5] influence of the nitrogen heteroatom. Both **5** and **8** show that the Fp^+ fragment is strongly displaced toward the α carbon,[13] supporting an enhanced contribution from resonance structure IV in the solid state.

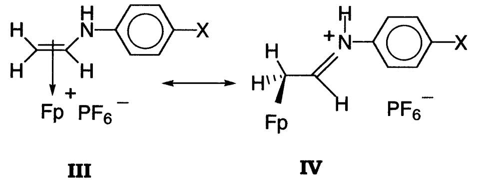

III **IV**

Comparing **5** and **8** to the previously reported structures of **2** and **3** shows that the extent of iron displacement along the face of the olefin lies between the methoxy olefin complex **2** and that of the dimethyl amino olefin complex **3**. Of note is the relative placement of **5** and **8** between the other two. The electron-withdrawing effect of the para acetyl substituent on **8** gives a δ value that is larger than that of **2**, yet shows a much less distorted structure than seen in **3**. Considering **8**, **5**, and **3** as a series with increasing electron density at nitrogen, it appears that this increase acts to displace the Fp^+ fragment toward the α carbon by stabilizing contributions from resonance structure IV. Such a displacement is also demonstrated by an opening of the $Fe-C\alpha-C\beta$ angle from 87.3° in **8** to an average of 94.1° in **5**. While these structures demonstrate significant displacement of the iron atom toward $C\alpha$, the observed $Fe-C\alpha-C\beta$ angles demonstrate that there remains a significant interaction with the olefin π system (particularly in the case of **8**). Hence, the α

---

(12) Structure **5a** in Table 1 shows a hydrogen bonding distance of 2.215 Å from the N−H to the F of the PF_6^- counterion. This interaction is not observed in **5b**, where the closest F to the N−H bond was 2.352 Å. This interaction and other crystal-packing forces result in a slight twisting of the aromatic ring, as well as the slight movement of the iron fragment. An overlay projection of the two structures is available in the Supporting Information.

(13) Comparisons given for **5** are based on the average bond lengths and angles for the two molecules in the asymmetric unit. The values in Table 1 clearly show that even the least distorted of the two molecules still is distinct from the structure of **8**.

carbon in both **5** and **8** is not a fully developed sp^3 center. The analogous angle in **3**[5] has opened to 104.2°, approaching that expected for a σ complex.

While the structures of both **5** and **8** show strong contributions from resonance structure IV, their relative position along the resonance continuum is expressed in geometry differences throughout the molecule. Given the trend in the δ parameters, it seems odd that the olefin bond length in both **5** and **8** should be equal to or shorter than that in **2**. Reported disorders[14] in the structure of **2** (particularly around C_α) cast some doubt on its reported olefin bond length. It is not surprising that the more electron-rich NMe_2 complex, **3**, displays a slightly longer olefin bond. This is supported by the fact that **3** has a shorter $C_\beta{-}N$ bond favoring an iminium structure. Comparison with structures **5** and **8** demonstrates that the para substituent directly influences the olefin bond length and the development of iminium character in the $C_\beta{-}N$ bond. Decreasing the electron donation from the para position upon moving from **5** to **8** results in a slight shortening of the olefin bond and a simultaneous lengthening of the $C_\beta{-}N$ interaction. This latter point supports the idea that the para substituent is directly influencing the interaction between the nitrogen lone pair and the β carbon of the olefin.

As the interaction between the nitrogen and the β carbon increases, one expects increasing planarity around nitrogen. The structures of **5** and **8** are strongly planar in this region. The bond angle (see Table 2) around nitrogen in **8** (C2−N−C21) is 127.2(2)° and has an average value of 127.9(5)° for the equivalent region of **5**, both revealing significant sp^2 character at nitrogen. In the structure of **8**, the dihedral angle between the olefin and nitrogen to aromatic ring bond (labeled C1−C2−N−C21 in the atom-numbering scheme of **8**) is −170.1°, while the average dihedral angle in the equivalent region of **5** is −173.0°. Worthy of note is the overall molecular planarity of **8** seen in Figure 3 (the hydrogen atoms have been omitted for greater clarity). This is reflected by the dihedral angle of −178.3° between the imine and the plane of the ring. In **5**, the average equivalent angle is −163.1°, showing a slight rotation of the bond between nitrogen and the aromatic ring. It would appear that the influence of the para acetyl group provides **8** with more extensive conjugation across the bulk of the molecule.

The structures of **5** and **8** argue that increasing the electron density on nitrogen allows for better overlap between the nitrogen lone pair and the β carbon and is directly related to the displacement of the Fp^+ fragment along the olefin face. This supports our contention that the position of the iron along the olefin face (and potentially the olefin reactivity) can be tuned by the controlling the relative energy of the heteroatom lone pair.

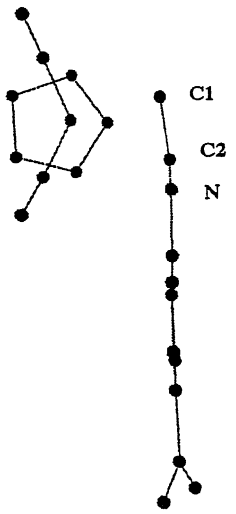

Figure 3. Side view of the structure of **8** showing the planar nature of the organic portion of the molecule. The PF_6^- counterion and the hydrogens have been removed for clarity.

Table 3. ^{13}C Shifts (ppm in CD_3NO_2) of the Olefin Carbons for Complexes 2−10, Relating Olefin Substitution to Displacement of the Fp^+ across the Olefin

complex (substituent)	C_α	C_β	δ
3[a] (NMe_2)	0.10	177.6	0.70 Å
4 (para OMe aniline)	8.94	163.8	
5 (para Me aniline)	9.88	161.9	0.50 Å
6 (para H aniline)	10.89	160.0	
7 (para Br aniline)	12.36	156.5	
8 (para COMe aniline)	14.70	151.2	0.35 Å
9 (para CN aniline)	16.34	147.4	
10 (para NO_2 aniline)	17.93	146.3	
2[a] (OMe)	27.30	146.2	0.23 Å

[a] See ref 16.

NMR Analysis and ^{13}C Hammett Study. The ^1H NMR data for the complexes reported here all show one remarkable feature. At room temperature, the olefinic proton resonances all show evidence of rotation about the olefin carbon−carbon bond. In place of the expected ABX system (cis, trans coupling across the double bond), the olefin protons form an A_2X spin system, giving a high-field doublet for the α protons and a low-field doublet of triplets (doublet splitting from coupling to adjacent N-H) for the β protons. The equivalency of the α protons is the result of carbon−carbon bond rotation facilitated by the rearrangement toward resonance structure IV. A facilitated bond rotation of this type was previously reported for **2**.[5] A description of the dynamic NMR properties of these complexes as well as a thorough measurement of the ΔH of activation for olefin bond rotation in several of these complexes is the subject of a subsequent publication.[15]

Carbon-13 NMR shifts for the olefinic carbons of this series are clearly sensitive to the electronic properties of the para substituent (see Table 3). Clearly the crystallography of complexes **3**, **5**, and **8** shows that nitrogen-substituted olefin complexes of Fp^+ are not symmetrically bound to the iron center. The symmetrically bound ethylene in $CpFe(CO)_2(C_2H_4)^+PF_6^-$ shows one olefin carbon resonance at 56.7 ppm.[16] The presence of the heteroatom and presumedly the interaction with its lone pair cause the two carbons to

---

(14) The crystal structure for complex **2** is disordered with respect to a mirror plane relating the α carbon to a carbonyl carbon. The authors report uncertainty in the Fe−Cα distance (see ref 5), which no doubt effects the reported C−C bond length. The authors note that this uncertainty would act to set a lower limit on the reported δ value of 0.12 Å, which would only strengthen the arguments presented above in the discussion of displacement of the Fp^+ fragment across the olefin face in response to electron density.

(15) Matchett, S. A.; Zhang, G. R. Manuscript in preparation.

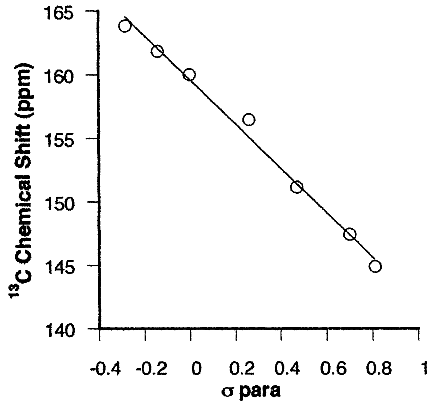

Figure 4. Correlation plot for ^{13}C chemical shift of olefin β carbon vs Hammett σ-para parameters for complexes **4**−**10**.

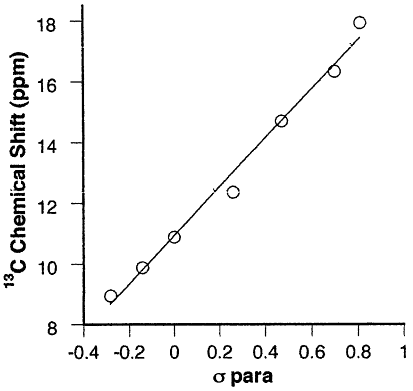

Figure 5. Correlation of the ^{13}C chemical shift of the α carbon vs Hammett σ para parameters for complexes **4**−**10**.

experience very different environments. While one could dismiss the changes in the ^{13}C shift of the β carbon from 56.7 ppm to be purely due to the inductive influence of an electronegative heteroatom, such a rationalization would not explain why **3** (N substituted) shows a larger downfield shift for the β carbon than does **2** (O substituted). We contend that it is the availability of the heteroatom lone pair for overlap with the β carbon that determines the chemical shift of the olefin carbons. The olefin ^{13}C chemical shifts for **4**−**10** fall between those seen for **2** and **3**. More significantly, changes in the para substituent on the ring directly influence the chemical shift of both carbons of the olefin. Included for comparison in Table 3 is the δ value from the known crystal structures as a measure of the displacement of the Fp^+ moiety along the olefin face. We feel that the electronic influence of the para substituent is changing the relative energy of the nitrogen atom lone pair and hence its ability to stabilize the shift of the iron toward the α carbon. As overlap between the heteroatom lone pair and the olefin fragment increases (increasing electron donation from the para substituent), the α carbon is shifted upfield while the β carbon resonance moves downfield. This offers additional experimental support for Rosenblum's argument originally based on the structures of **2** and **3**. It should be noted that the para nitro derivative, **10**, shows ^{13}C shifts for the olefin carbons that are approaching those of the OMe derivative, **2**.

The usefulness of Hammett[17] σ constants to explore the correlation between electron structure and chemical structure/reactivity is well established. Specifically, correlation of σ parameters to NMR chemical shifts is also precedented.[18] When the Hammett σ_{para} coefficient for each of the para substituents is plotted against the^{13}C chemical shifts of the β carbon, the plot (Figure 4) is seen to be linear with a correlation coefficient of 0.992 for seven data points. Correlation coefficients greater than 0.95 are considered to show a significant correlation between NMR chemical shifts and Hammett σ values.[18a] The value of ρ equals −16.72, corresponding to an increase in the chemical shift of the β carbon as the electron-releasing ability of the para group increases. As the electron-donating character of the para substituent increases, we feel there is greater overlap of the nitrogen lone pair with the β carbon LUMO, favoring displacement of the iron fragment toward the α carbon. This results in an increased contribution from resonance structure IV. When the para substituent is electron withdrawing, the overlap decreases and the structure reflects an increased contribution from resonance structure III.

An obvious choice in a study of this type is the para NH_2 derivative made from phenylene diamine. While this derivative forms readily, the ^{13}C shift for the β carbon of 165.5 ppm lies well below the correlation line given in Figure 4. The ^{1}H NMR for this derivative varies with the concentration of the solution. At increasing concentrations, the spectrum shows no downfield doublet for the N-H peak on the olefin. Instead, a broad upfield resonance of variable chemical shift integrates to approximately three protons. We attribute this to an acidity of the olefin-bound N-H caused by a significant contribution from resonance structure IV in the presence of the strong para electron-donating NH_2 group. In addition to favoring resonance structure IV, the presence of the para NH_2 group provides a convenient proton acceptor site. The proton transfer is not complete since the correlation with the σ_{para} for an NH_3^+ group ($\sigma_{\text{para}} = 0.60$) still lies well off the correlation line. The ^{13}C shift for the β carbon of this derivative is less than that expected for a para NH_2 group and much larger than expected for a para NH_3^+ group. The observed resonance in the ^{1}H NMR represents the time-averaged exchange between the acid and base sites. The collapse of the downfield doublet for the olefinic N-H with increasing concentration may imply a bimolecular process, although a kinetic analysis has not yet been performed.[19]

A similar plot (Figure 5) can be constructed comparing the Hammett σ_{para} coefficients to the ^{13}C α carbon shifts. A linear correlation to the electronic nature of the para substituent is again observed; however, the fit is not quite as good ($R^2 = 0.988$ for 7 data points). The positive value of ρ (+8.19) shows a decrease in chemical shift as

---

(16) Substituted Olefin Complexes of Cyclopentadienyldicarbonylrion: Structure and Spectroscopic Properites: Stockman, C. T. Ph.D. Thesis, Brandeis University, Waltham, MA, 1986, and the data therein.

(17) Hammett, L. P. *J. Am. Chem. Soc.* **1937**, *59*, 96.

(18) (a) Ewing, D. F. Correlation of NMR Chemical Shifts with Hammett σ Values and Analogous Parameters. In *Correlation Analysis in Chemistry*: *Recent Advances*; Chapman, N. B., Shorter, J., Eds.; Plenum Press: New York, 1978. (b) Malet, R.; Marcial, M. M.; Parella, T.; Pleixats, R. *Organometallics* **1995**, *14*, 2463.

(19) Work to determine the ΔH of activation for proton transfer using peak width at half-height techniques is ongoing in our lab.

the electron-releasing properties of the para substituent increase. This is consistent with the proposed displacement of the Fp^+ fragment toward the α carbon and the developing sp^3 character there.

Attempts to correlate ^{13}C shifts for the α, β, or carbonyl carbons with either σ^+ or σ^- values failed to produce significant linear agreement. Failure of the σ^+ value, despite the positive charge in the molecule is reasonable given that the dominance of resonance structure IV should place the majority of the plus charge on the nitrogen atom.

This study demonstrates that changes in the electron-donating/-withdrawing properties of the para substituent can be used to control the displacement of the Fp^+ fragment along the olefin face. Since it has been theorized that this displacement is directly related to the reactivity toward nucleophilic substitution in these complexes, such control should also extend to reactivity in the series. It was previously demonstrated that small ground state displacements strongly favored substitution, while large displacements effectively prevented the reaction. Since reactivity cannot be thought of in terms of an on/off switch, there must exist a transition between these extremes as the Fp^+ is displaced along the olefin face. Work in our group is underway to assess the relative reactivity of each of these complexes with a common nucleophile in an effort to correlate this reactivity to the ^{13}C shift of the β carbon of the coordinated olefin. While many factors determine the final ^{13}C shift in the NMR, such a correlation could develop into a useful tool for predicting relative susceptibility to nucleophilic attack in metal olefin complexes.

Experimental Section

General Procedures. All reactions were carried out under N_2 using standard Schlenk line techniques. Solvents were distilled under a N_2 atmosphere off of appropriate drying and/or deoxygenating reagents (CH_2Cl_2, CaH_2; Et_2O, Na/benzophenone). CD_3NO_2 was dried on P_2O_5 and distilled by vacuum transfer prior to use. CD_3NO_2 NMR tubes were prepared in an inert atmosphere glovebox. CD_3COCD_3 was dried on 3 Å molecular sieves and vacuum transferred directly into the NMR tube. NMR spectra were recorded on a JEOL Eclipse 300 at 300.52 MHz for ^1H and 75.57 MHz for ^{13}C. All chemical shifts were referenced to the residual protons in the deuterated solvents. Vinylic carbon ^{13}C shift assignments used in the Hammett plots were confirmed using an HMQC NMR experiment. Values for the various σ parameters were obtained from the text *Advanced Organic Chemistry*.[20] Samples of the ethyl vinyl ether starting material, $CpFe(CO)_2(CH_2CHOEt)^+PF_6^-$, were prepared by reported literature methods.[7] All para-substituted anilines were sublimed prior to use. Elemental analyses were performed by Galbraith Laboratories, Knoxville, TN. As cations, these Fp^+ salts tend to retain solvent (particularly diethyl ether), making elemental analysis more difficult. As complexes **4**−**10** represent an analogous series, successful analyses for **4**, **6**, **7**, and **10** were taken as confirmation for the series.

Typical Procedure for the Preparation of para-Substituted Aniline Complexes of the $CpFe(CO)_2^+$ Cation. To a solution of $CpFe(CO)_2(CH_2CHOEt)^+PF_6^-$ (0.200 g, 0.508 mmol) in CH_2Cl_2 (10 mL) was added a 10 mol % excess of the para-substituted aniline species as a solution in 4 mL of CH_2Cl_2. The resulting orange solution was stirred at room temperature for 2−4 h. The length of time was increased as the nucleophilicity of the aniline species decreased. As the reaction proceeded, the ionic product began to precipitate from solution as a dark red-orange powder. The solvent from the reaction mixture was then reduced under vacuum, and diethyl ether was added to complete precipitation. The residue was then recrystallized from dichloromethane and diethyl ether. The resulting powder was isolated by filtration and dried under vacuum to give respectively **4** (43.0% isolated yield), **5** (70.3% isolated yield), **6** (62.1% isolated yield), **7** (50.2% isolated yield), **8** (59.7% isolated yield), **9** (50.1% isolated yield), and **10** (67.1% isolated yield).

Characterization Data for *p*-OMe Derivative 4. ^1H NMR (acetone-d_6, 300.53 MHz): 2.49 (d, 2 H, J = 8.5 Hz, olefin CH_2), 5.30 (s, 5 H, Cp), 7.06 (d, 2 H, J = 7.7 Hz, aromatic), 7.38 (d, 2 H, J = 7.7 Hz, aromatic), 8.43 (d of t, 1 H, J_{H-NH} = 14.6 Hz J = 9.1 Hz, olefin CHN), 9.30 (br d, 1H, J = 12.0 Hz, NH). $^{13}C\{^1H\}$ (nitromethane-d_3, 75.58 MHz): δ 8.9 (olefin CH_2), 87.4 (CH_{Cp}), 116.6, 121.5 (CH aromatic), 131.9, 160.6 (C aromatic), 163.8 (olefin CHN), 214.3 (CO) ppm. IR (KBr): 2002, 2042 cm^{-1}. Anal. Calcd for $C_{16}H_{16}NO_3F_6FeP$: C, 40.791; H, 3.423; N, 2.973. Found: C, 40.76; H, 3.35; N, 3.04.

Characterization Data for *p*-Me Derivative 5. ^1H NMR (acetone-d_6, 300.53 MHz): δ 2.54 (d, 2 H, J = 9.1 Hz, olefin CH_2), 5.32 (s, 5 H, Cp), 7.34 (s, 4 H, aromatic), 8.48 (d of t, 1 H, J_{H-NH} = 15.0 Hz J = 8.6 Hz, olefin CHN), 9.28 (br d, 1H, J = 13.7 Hz, NH). $^{13}C\{^1H\}$ (nitromethane-d_3, 75.58 MHz): δ 9.9 (olefin CH_2), 87.4 (CH_{Cp}), 119.7, 132.0, (CH aromatic), 136.4, 139.5 (C aromatic), 161.9 (olefin CHN), 214.1 (CO) ppm. IR (KBr): 1992, 2048 cm^{-1}.

Characterization Data for *p*-H Derivative 6. ^1H NMR (acetone-d_6, 300.53 MHz): δ 2.57 (d, 2 H, J = 9.1 Hz, olefin CH_2), 5.33 (s, 5 H, Cp), 7.33−7.60 (mult., 4 H, aromatic), 8.49 (d of t, 1 H, J_{H-NH} = 15.1 Hz J = 8.9 Hz, olefin CHN), 9.13 (br d, 1H, J = 14.0 Hz, NH). $^{13}C\{^1H\}$ (nitromethane-d_3, 75.58 MHz): δ 10.9 (olefin CH_2), 87.5 (CH_{Cp}), 119.7, 131.6 (CH aromatic), 128.7, 138.9 (C aromatic), 160.0 (olefin CHN), 213.9 (CO) ppm. IR (KBr): 2001, 2039 cm^{-1}. Anal. Calcd for $C_{15}H_{14}NO_2F_6FeP$: C, 40.85; H, 3.20; N, 3.17. Found: C, 40.81; H, 3.20; N, 3.18.

Characterization Data for *p*-Br Derivative 7. ^1H NMR (acetone-d_6, 300 MHz): δ 2.69 (d, J = 9.1 Hz, olefin CH_2), 5.55 (s, 5 H, Cp), 7.51 (d, 2 H, J = 9.0 Hz, aromatic), 7.69 (d, 2 H, J = 9.0 Hz, aromatic), 8.87 (d of t, 1 H, J_{H-NH} = 14.3 Hz J = 9.1 Hz, olefin CHN), 10.63 (br d, 1H, J = 11.3 Hz, NH). $^{13}C\{^1H\}$ (nitromethane-d_3, 75.58 MHz): δ 12.4 (olefin CH_2), 87.6 (CH_{Cp}), 121.3, 131.6, (CH aromatic), 121.0, 134.4 (C aromatic), 156.5 (olefin CHN), 213.9 (CO) ppm. IR (KBr): 2002, 2052 cm^{-1}. Anal. Calcd for $C_{15}H_{13}NO_2FeBrPF_6$: C, 34.65; H, 2.52; N, 2.69. Found: C, 34.32; H, 2.45; N, 2.65.

Characterization Data for *p*-COMe Derivative 8. ^1H NMR (acetone-d_6, 300 MHz): δ 2.78 (br d, J = 8.26 Hz, olefin CH_2), 5.59 (s, 5 H, Cp), 7.63 (d, 2 H, J = 8.8 Hz, aromatic), 8.11 (d, 2 H, J = 8.8 Hz, aromatic), 8.91 (d of t, 1 H, J_{H-NH} = 14.3 Hz, J = 9.2 Hz, olefin CHN), 10.51 (br d, 1H, J = 13.8 Hz, NH). $^{13}C\{^1H\}$ (nitromethane-d_3, 75.58 MHz): δ 14.7 (olefin CH_2), 26.8 (CH_3), 87.7 (CH_{Cp}), 118.9, 131.8 (CH aromatic), 136.3, 142.8 (C aromatic), 151.2 (olefin CHN), 198.8 (CO of acetyl), 213.1 (CO) ppm. IR (KBr): 2000, 2043 cm^{-1}.

Characterization Data for *p*-CN Derivative 9. ^1H NMR (acetone-d_6, 300.53 MHz): δ 2.76 (d, 2 H, J = 9.4 Hz, olefin CH_2), 5.42 (s, 5 H, Cp), 7.52 (d, 2 H, J = 8.8 Hz, aromatic), 7.84 (d, 2 H, J = 8.5 Hz, aromatic), 8.38 (d of t, 1 H, J_{H-NH} = 14.3 Hz, J = 9.4 Hz, olefin CHN), 8.71 (br d, 1H, J = 14.0 Hz, NH). $^{13}C\{^1H\}$ (nitromethane-d_3, 75.58 MHz): δ 16.3 (olefin CH_2), 87.9 (CH_{Cp}), 119.4, 135.6, (CH aromatic), 110.5, 143.0 (C aromatic), 147.4 (olefin CHN) ppm. CN carbon not located.[21] Fe-CO peak(s) not located due to dynamic exchange.[22] IR (KBr): 2009, 2052, 2234 cm^{-1}.

---

(20) March, J. *Advanced Organic Chemistry*; Wiley and Sons: New York, 1985; p 244.

Table 4. Experimental Data for the Crystal Structures of 5 and 8

	5	**8**
empirical formula	$C_{16}H_{16}F_6FeNO_2P$	$C_{17}H_{16}F_6FeNO_3P$
fw	455.12	483.13
temperature	120 K	233 K
wavelength	1.54178 Å	0.71073 Å
cryst syst	triclinic	orthorhrombic
space group	$P2_1/n$	$Pna2_1$
unit cell dimens	$a = 17.9949(6)$,	$a = 15.095(3)$,
	$\alpha = 90°$	$\alpha = 90°$
	$b = 10.5648(3)$,	$b = 7.2282(17)$,
	$\beta = 95.033(2)°$	$\beta = 90°$
	$c = 19.1257(7)$,	$c = 17.975(4)$,
	$\gamma = 90°$	$\gamma = 90°$
volume (Å^3)	3622.0(2)	1961.2(8)
Z	8	4
density(calc)	1.669 Mg/m^3	1.636 Mg/m^3
abs coeff	8.194 mm^{-1}	0.924 mm^{-1}
F(000)	1840	976
θ range for collection	3.23 to 59.21°	2.27 to 28.24°
no. of reflns collected	12071	12898
no. of indep reflns	4124	4332
data, $I > 2\sigma(I)$	3045	4332
no. of params/restraints	490/0	4332/343
R1, wR2 (all data)	0.0710, 0.1395	0.0465, 0.0677
R1, wR2 [$I > 2\sigma(I)$]	0.0505, 0.1245	0.0311, 0.0637
GOF on F^2	1.039	1.061

Characterization Data for *p*-NO_2 Derivative 10. ^{1}H NMR (acetone-d_6, 300 MHz): δ 2.83 (d, 2 H, $J = 6.9$ Hz, olefin CH_2), 5.44 (s, 5 H, Cp), 7.55 (d, 2 H, $J = 6.3$ Hz, aromatic) 8.34, (d with broad base, 3H, $J = 6.3$ Hz, aromatic with 1 olefin CH overlapping base), 8.62 (br d, 1H, $J = 10.2$ Hz, NH). ^{13}C-{^{1}H} (nitromethane-d_3, 75.58 MHz): δ 17.9 (olefin CH_2), 88.0 (CH_{Cp}), 118.9, 143.8, (CH aromatic), 127.2, 143.8 (C aromatic), 146.3 (olefin CHN) ppm. Fe-CO peak(s) not located due to dynamic exchange.[19] IR (KBr): 2015, 2060 cm^{-1}. Anal. Calcd for $C_{15}H_{14}N_2O_4F_6FeP$: C, 37.06; H, 2.70; N, 5.76. Found: C, 37.11; H, 2.67; N, 5.76.

Crystallography on 5.[23] The data were collected on a Bruker SMART 6K CCD X-ray area detector with a window diameter of 13.5 cm. It was controlled by a Windows 2000 based PC computer with SMART version 5.625 software (Bruker, 2001), at low temperature (120 K), with graphite-monochromatized Cu Kα radiation [λ(Cu Kα) = 1.54184 Å]. All reflections were measured in image groups with 606 frames in each group, and the exposure time was 5 s per frame. Among them, three groups of images were collected at $2\theta = -40°$, and the other three groups were at $2\theta = -80°$, which makes the $2\theta_{max} = 133.07°$. The data reduction program SAINT+ version 6.22 (Bruker 2001) determined the Laue group was $2/m$, and a total of 4124 unique reflections were integrated for structure solution and refinements. The space group was $P21/m$. The structure was solved by direct methods using SHELXS version 6.12 (Bruker, 2001). The trial solution obtained 54 non-hydrogen atoms in the asymmetrical unit. Least-squares refinement included all non-hydrogen atomic coordinates and anisotropic thermal parameters. With two molecules in the asymmetric unit, the final refinement cycle gave, with 3045 reflections with intensities > $2\sigma(I)$: $R = 0.0505$, $R_w{}^2 = 0.1245$; with all 4121 reflections: $R = 0.0710$. The hydrogen atoms were placed in calculated positions. Key crystallographic constants and parameters are given in Table 4.

Crystallography on 8.[24] X-ray diffraction data were collected on a Bruker P4 diffractometer equipped with a SMART CCD detector, and crystal data, data collection, and refinement parameters are summarized in Table 4. A total of 4332 unique reflections were integrated for structure solution and refinement. The structures were solved using direct methods and standard difference map techniques and were refined by full-matrix least-squares procedures on F^2 with SHELXTL (Version 6.10). The final refinement cycle, with 4332 reflections with intensities $>2\sigma$, gave $R = 0.0311$, $R_w{}^2 = 0.0637$ and $R = 0.0465$ with all reflections. The hydrogen atoms were placed in calculated positions. Key crystallographic constants and parameters are given in Table 4.

Acknowledgment. Thanks are expressed to the Michigan Space Grant Consortium, the Council on Undergraduate Research, and the Grand Valley State University Summer Undergraduate Research Program for their financial support of this work. Special thanks to the laboratories of Dr. Gerald Parkin (Columbia University, New York) for performing the X-ray crystal structure determination of **8** and to the laboratories of Pfizer Corporation (Kalamazoo, MI) and in particular Garold Bryant, Jr. for performing the X-ray crystal structure determination of **5**.

Supporting Information Available: Listings of the atomic coordinates, bond lengths, bond angles, anisotropic displacement parameters, hydrogen coordinates, and anisotropic displacements for the crystal structures of **5** and **8** are available. In addition, an overlay projection of the two molecules in the asymmetric unit of **5** is available. This material can be obtained free of charge via the Internet at http://pubs.acs.org.

OM0305566

---

(21) ^{13}C run with up to a 6 s relaxation delay. Peak expected at about 118 or 119 ppm based on aromatic nitriles and may lay beneath the peak at 119.4 ppm.

(22) Work on the dynamic behavior of these molecules by our lab is demonstrating that as the electron-withdrawing properties of the para substituent increase, the dynamic process that equilibrates the two metal carbonyls slows down. At room temperature, these peaks for complexes **9** and **10** appear to have coalesced. Manuscript in preparation.

(23) Structure performed as a courtesy of Garold L. Byrant at the X-ray structure facilities of Pfizer in Kalamazoo, MI. See acknowledgments.

(24) The structure was performed as a courtesy by the research group of Gerald Parkin, Department of Chemistry, Columbia University, New York. See acknowledgments.